

Analysis and Evaluation of MB-OFDM Dual Carrier Modulation

Darryn Lowe and Xiaojing Huang

Telecommunications Information Technology Research Institute

University of Wollongong

Northfields Avenue, Australia 2522

{darrynl, huang}@uow.edu.au

Abstract—In this paper, we investigate the dual carrier modulation (DCM) proposed for use in the multi-band orthogonal frequency division multiplexing (MB-OFDM) ultra-wideband (UWB) standard. DCM obtains a significant diversity improvement by spreading coded information bits on non-adjacent subcarriers. By considering DCM as a realization of block-spread OFDM (BS-OFDM), we show that DCM performs well against comparable spreading matrices. We also explore the relationship between DCM and constellation order to conclude that the MB-OFDM packet error rate performance can be further improved by adjusting the puncturing pattern and modulation order.

I. INTRODUCTION

Ultra-wideband (UWB) communication systems are of great interest due to their support for high data rates and their resistance to interference [1]. With UWB officially defined in 2002 by the United States *Federal Communications Commission* (FCC) as a signal with a 10 dB bandwidth of at least 500 MHz and a maximum equivalent isotropic radiated *power spectral density* (PSD) of no more than -41.3 dBm/MHz in the 3.1 – 10.6 GHz band [2], the race is on to exploit this untapped spectral resource.

The first UWB technology to be internationally standardized is *multi-band orthogonal frequency division multiplexing* (MB-OFDM) [3] developed by the WiMedia Alliance. The MB-OFDM standard includes both an UWB *physical layer* (PHY) and *medium access control* (MAC) and supports data rates from 53.3 Mbps to 480 Mbps. MB-OFDM divides the several gigahertz of spectrum allocated by the FCC into 14 bands, each with a 528 MHz bandwidth. These bands are then bundled into 5 band groups with only the first mandatory.

MB-OFDM, which shares the generic OFDM block diagram of Fig. 1, has four distinguishing characteristics from previous OFDM *wireless local area network* (WLAN) standards such as IEEE 802.11a/g and HiperLAN/2. First, an MB-OFDM symbol is comprised of 128 samples rather than the 64 samples used in IEEE 802.11a. Second, a *zero-pad* (ZP) is used rather than a *cyclic prefix* (CP). Although a ZP leads to a higher peak-to-average power ratio, it is more efficient than a CP since there is not wasted energy. Third, MB-OFDM supports a range of optional diversity improvements. This includes *frequency domain spreading* (FDS) and *time domain spreading* (TDS), both of which offer an extra 3 dB of process gain when activated, as well as *dual carrier modulation* (DCM) to

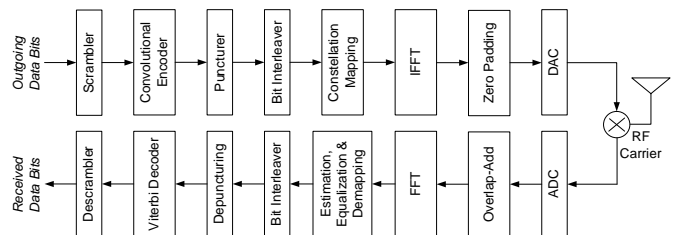


Fig. 1. Block diagram of an MB-OFDM transceiver.

combat frequency selective fading at high data rates. Fourth, *time-frequency codes* (TFCs) support optional *time-frequency interleaving* (TFI) to yield up to a 4.7 dB increase in transmit power. This is possible since as each 528 MHz band is only active for 1/3 of the time, the average power radiated per-band can be up to 3 times higher without violating the -41.3 dBm/MHz FCC limit.

To support data rates of 320 Mbps or higher, the MB-OFDM standard needs to send up to 1.5 coded information bits per OFDM subcarrier. This means that the TDS and FDS techniques used at low rates are too costly and can not be used. Further, with the convolutional coding rate reduced to as little as $R = \frac{3}{4}$, it is difficult for the high rates to recover from deep fades in the frequency-selective UWB channel. To mitigate the extent of this problem, without reducing data rate, DCM was proposed in [4] to increase diversity at the expense of receiver complexity.

In this paper we analyze the performance of DCM and evaluate it against alternative means of increasing diversity for the OFDM system defined in Section II. Section III begins the analysis by examining the theoretical uncoded performance of DCM-type diversity techniques in frequency-selective UWB channels. We then expand on these results to consider the theoretical capacity and effective *packet error rate* (PER) of a coded MB-OFDM system in Section IV. Finally, we conclude and provide our recommendations in Section V.

II. DUAL CARRIER MODULATION

We model an OFDM system as

$$\mathbf{y} = \mathbf{H}\mathbf{q} + \mathbf{n} \quad (1)$$

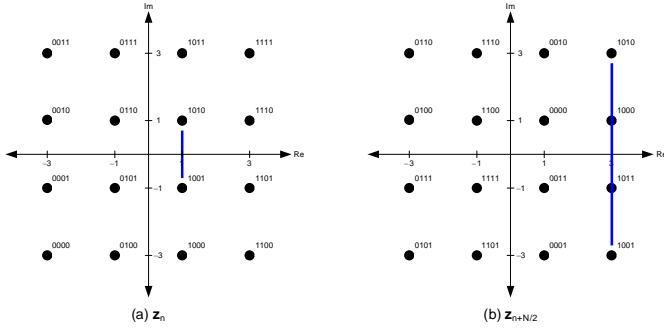


Fig. 2. DCM constellations.

where \mathbf{y} is the received vector post-FFT, $\mathbf{H} = \text{diag}(\mathbf{h})$ and is a diagonal matrix of the vector of complex channel fading coefficients \mathbf{h} , $\mathbf{q} \in \mathcal{A}^N$ and is the vector of transmitted data symbols, with each symbol drawn from the alphabet \mathcal{A} , and \mathbf{n} is a vector of independent and identically distributed zero-mean Gaussian noise with variance N_0^2 . Without loss of generality, we assume that the channel fading coefficients and symbol alphabet \mathcal{A} are normalized such that $E[|\mathbf{h}_n^2|] = 1$ and $E[|\mathbf{q}^2|] = 1$ respectively.

At data rates less than 320Mbps, the data symbol vector \mathbf{q} is obtained using a *quadrature phase shift keying* (QPSK), referred to hereafter as 4QAM, mapping of the convolutionary-coded information bits. Since each bit is localized to a single symbol, the main protection against frequency-selective fading is the FEC. Unfortunately, the aggressive puncturing needed to obtain the higher data rates reduces the effectiveness of the *forward error correction* (FEC).

To mitigate the impact of frequency-selective fading without reducing the data rate, DCM was added to the MB-OFDM standard [4]. By modulating data symbols in pairs, DCM adds frequency diversity and thereby reduces the dependence on the FEC. The DCM constellation pair defined by the MB-OFDM standard is shown in Fig. 2. Note that the pair of DCM constellations denotes 4 information bits; the data rate is therefore the same as conventional 4QAM. We observe that in addition to spreading the energy of each coded information bit over two symbols, the constellation mappings are defined such that neighboring codewords in one constellation are further apart in the other.

Assuming that the each constellation point is equally probable, optimal reception is achieved by producing soft-decision *log-likelihood ratio* (LLR) decision variables via a *maximum likelihood* (ML) detector. If we denote the Euclidean distance for each symbol vector as

$$\delta^2 = \|\mathbf{y} - \mathbf{H}\mathbf{q}\|^2 \quad (2)$$

then we can define the ML LLR as

$$\hat{\lambda}_{\text{ML}}^{(k)} = \log \left(\frac{\sum_{\delta^2 \in D_k^+} \exp\left(-\frac{\delta^2}{N_0^2}\right)}{\sum_{\delta^2 \in D_k^-} \exp\left(-\frac{\delta^2}{N_0^2}\right)} \right) \quad (3)$$

where D_k^+ and D_k^- denote the set of all possible symbol vectors where the k^{th} information bit is +1 and -1 respectively. Since the complexity of an ideal ML detector can be prohibitive, a common simplification is

$$\hat{\lambda}_{\text{ML}}^{(b)} = \frac{1}{N_0^2} \left(\arg \min_{\delta^2 \in D_k^-} - \arg \min_{\delta^2 \in D_k^+} \right) \quad (4)$$

This latter approach readily lends itself to low-complexity implementation via sphere decoding [5].

III. ANALYSIS OF UNCODED DCM

DCM is a member of the family of OFDM diversity improvement techniques that we term *block-spread OFDM* (BS-OFDM) [6]. The objective of this section is to evaluate the *bit error rate* (BER) of DCM relative to other forms of BS-OFDM.

In all BS-OFDM systems, the N subcarriers of the original OFDM symbol are grouped into $\frac{N}{M}$ blocks of M subcarriers. Each block is then spread by a square $M \times M$ matrix \mathbf{U} . Since the goal is to increase frequency diversity, the subcarriers in each block are usually selected to maximize their frequency separation. We can therefore denote a single BS-OFDM block of order M as

$$\mathbf{z} = \mathbf{H}_M \mathbf{U} \mathbf{q}_M + \mathbf{n}_M \quad (5)$$

where

$$\mathbf{H}_M = \begin{bmatrix} \mathbf{h}_0 & 0 & \dots & 0 \\ 0 & \mathbf{h}_{\frac{N}{M}} & \dots & 0 \\ \vdots & \vdots & \ddots & \vdots \\ 0 & 0 & \dots & \mathbf{h}_{\frac{mN}{M}} \end{bmatrix} \quad (6)$$

and

$$\mathbf{q}_M = \begin{bmatrix} \mathbf{q}_0 \\ \mathbf{q}_{\frac{N}{M}} \\ \vdots \\ \mathbf{q}_{\frac{mN}{M}} \end{bmatrix} \quad (7)$$

where $0 \leq m < M$ and similarly for \mathbf{n}_M . Although we only explicitly consider the case where N is an integer multiple of M , we incur no loss of generality doing so since N is easily adjustable by designating some subcarriers as pilots. For example, in the MB-OFDM standard, only 100 of the original $N = 128$ subcarriers are used to transfer data.

An upper bound [7] on the probability of bit error for BS-OFDM in a known channel is given by

$$P_{e|\mathbf{H}_M} \leq \sum_{\mathbf{e}_k \in \varepsilon_M} Q \left(\frac{\|\mathbf{H}_M \mathbf{U} \mathbf{e}_k\|}{N_0} \right) \quad (8)$$

where \mathbf{e}_k denotes the k^{th} element of ε_M , with ε_M denoting a set that encapsulates all errors for a given block of size M . In other words,

$$\varepsilon = \{\mathbf{a} - \mathbf{b} | \mathbf{a} \in \mathcal{A}^M \text{ and } \mathbf{b} \in \mathcal{A}^M\} \quad (9)$$

For example, when \mathcal{A} denotes 4QAM and $M = 1$, ε contains 16 elements. Alternatively, when $M = 2$, the cardinality of ε will be 256. Since many of the elements of ε are not unique, it

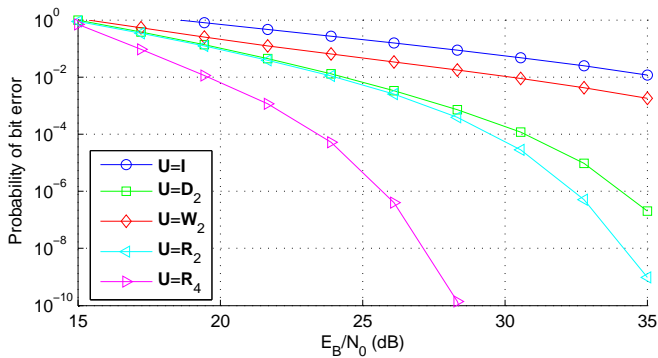


Fig. 3. Frequency-selective BER of BS-OFDM for various block spreading matrices.

is possible to speed a numeric analysis of (9) by pre-processing to group like terms [8].

It is apparent from (5) that the block spreading matrix \mathbf{U} determines the degree of any diversity gain. For example, if \mathbf{U} is the identity matrix \mathbf{I} , BS-OFDM is equivalent to conventional OFDM with a permuted symbol vector. This case is used to as a reference in many of the following analyses. As BS-OFDM aim to increase frequency diversity, no BS-OFDM technique can improve performance in a flat-fading purely-AWGN channels. Further, if the block spreading matrix does not satisfy $\mathbf{U}^H \mathbf{U} = \mathbf{I}$, where \mathbf{U}^H denotes the Hermitian transpose of \mathbf{U} , AWGN performance will be degraded. This is because energy will no longer be evenly distributed over all data symbols in the block.

For uncoded frequency-selective channels, we can evaluate the performance of a given block spreading matrix in terms of its expected BER by averaging (8) over all possible channels. In this paper, we focus on the short-range non-line-of-sight ‘CM2’ channel model from the IEEE 802.15.3a working group [9]. All IEEE UWB channel models are based on a the *Salem-Venezuela* (S-V) model and are parameterized to consider the clustering phenomena common to UWB channels. Note that we simplify our numerical analyses by normalizing each channel realization. In other words, we disregard the shadowing effects normally considered by the IEEE channel models since we evaluate performance as a function of SNR and not distance.

Results comparing the performance of several block spreading matrices are shown in Fig. 3. The first block spreading matrix that we consider denotes MB-OFDM DCM and is defined as

$$\mathbf{D}_2 = \frac{1}{\sqrt{5}} \begin{bmatrix} 2 & 1 \\ 1 & -2 \end{bmatrix} \quad (10)$$

The second block spreading matrix is a normalized $M \times M$ Walsh-Hadamard matrix. For example, the well-known $M = 2$ case is

$$\mathbf{W}_2 = \frac{1}{\sqrt{2}} \begin{bmatrix} 1 & 1 \\ 1 & -1 \end{bmatrix} \quad (11)$$

The third and final type of spreading matrix we consider is

the rotated Walsh-Hadamard family [6]

$$\mathbf{R}_M = \mathbf{W}_M \text{diag}\{\alpha_m\} \quad (12)$$

where $\alpha_m = e^{\frac{j\pi m}{C}}$. It is found in [8] that the optimal C causes $\frac{2\pi}{C}$ to denote the smallest angle that rotates the symbol alphabet \mathcal{A} back onto itself. In the case of 4QAM, this means that $C = 4$.

Examination of Fig. 3 shows that DCM, Walsh-Hadamard and rotated Walsh-Hadamard matrices all offer improvements over conventional OFDM. It is expected that the Walsh-Hadamard matrix shows the smallest improvements since there are some 4QAM symbol vectors that lead to zeros after spreading. For example, if

$$\mathbf{q}'_2 = \frac{1}{\sqrt{2}} \begin{bmatrix} 1 + j \\ 1 + j \end{bmatrix} \quad (13)$$

then the spread symbol vector

$$\mathbf{W}_2 \mathbf{q}'_2 = \begin{bmatrix} 1 + j \\ 0 \end{bmatrix} \quad (14)$$

will localize all energy to a single subcarrier. This is counter-productive given that our objective is to increase frequency-diversity. We conclude that Walsh-Hadamard spreading matrices should therefore be avoided.

Fig. 3 also shows there is relatively little difference between DCM and the similarly-sized $M = 2$ rotated Walsh-Hadamard matrix. This is particularly evident at low SNR. Although the larger $M = 4$ rotated Walsh-Hadamard matrix is superior, the complexity involved in processing such a large block spreading matrix at the receiver is prohibitive. Indeed, in terms of complexity, DCM is superior to the rotated Walsh-Hadamard matrix since the DCM spreading matrix is purely real and thereby avoids any complex multiplications. Our overall conclusion is that DCM is an effective realization of BS-OFDM and that it performs well in uncoded frequency-selective UWB channels.

IV. ANALYSIS OF CODED DCM

Almost all practical OFDM systems use FEC, with the most common realization being convolutional coding at the transmitter and Viterbi decoding at the receiver. This spreads information bits over multiple subcarriers and thereby increases robustness against frequency-selective fading. In MB-OFDM, a fixed-rate $R = \frac{1}{3}$ convolutional code is used from which multiple data rates are derived via variable puncturing patterns.

Fig. 4 shows the results of a Monte Carlo simulation of the PER for a 480Mbps MB-OFDM system with 1500 octet packets in a CM2 channel with ideal ML detection as per (3). To obtain a 480Mbps data rate, MB-OFDM punctures the underlying $R = \frac{1}{3}$ convolutional code down to $R = \frac{3}{4}$. Given that the final coding gain is relatively small, it is to be expected that the diversity improvements of BS-OFDM should be similar to those of the uncoded system considered previously.

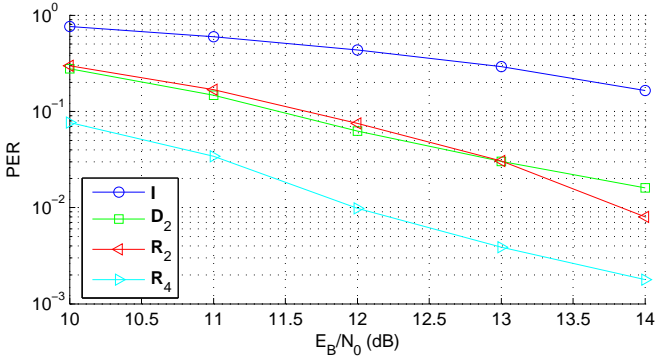


Fig. 4. PER at 480Mbps in CM2 relative to choice of BS matrix.

Although Fig. 4 demonstrates the relative effectiveness of DCM as one realization of BS-OFDM, it does not compare DCM to other forms of coding. To that end, we denote the capacity of the channel in terms of its cut-off rate [7] as

$$R_0(\mathbf{H}) = -\frac{1}{M} \log_2 \left(\frac{1}{|\varepsilon|^2} \sum_{\mathbf{e}_k \in \varepsilon} \exp \left\{ -\frac{\|\mathbf{H}\mathbf{U}\mathbf{e}_k\|^2}{4N_0} \right\} \right) \quad (15)$$

where $|\varepsilon|$ is the cardinality of the set of error vectors ε . The expected capacity R_0 is obtained by averaging $R_0(\mathbf{H})$ over the set of expected channels, similar to what was done for (8) in the previous section.

Fig. 5 shows the cut-off rate of the CM2 channel for several modulations and block spreading matrices. In other words, we different combinations of rotated Walsh-Hadamard block spreading matrices, with $M = \{1, 2, 4\}$, and symbol alphabets, with $\mathcal{A} = \{4\text{QAM}, 8\text{QAM}, 16\text{QAM}\}$. Note that although a rotated Walsh-Hadamard matrix is necessary in order to consider $M > 2$, the results are readily applicable to DCM given that Fig. 3 shows relatively little difference between the two techniques.

We observe from Fig. 5 that there is a more rapid increase in channel capacity for larger block spreading matrices. This is particularly noticeable when N_0 is less than 15 dB. We also observe that increasing the constellation order from 4QAM to 8QAM is superior to applying $M = 2$ block spreading. Although $M = 4$ block spreading slightly outperforms unspread 8QAM at low SNR, the 2 bits/dimension asymptotic limit makes 8QAM the preferred choice for higher SNRs.

To determine the most efficient modulation for real-world systems, the complexity of implementation must be considered. As the complexity of a ML detector is proportional to the cardinality of the set of transmitted symbols, Table I considers the number of states denoted by the vector $\mathbf{U}\mathbf{q}$ for each scenario of Fig. 5. It is apparent that although BS-OFDM increases robustness to frequency-selective fading for all symbol alphabets, the number of states needed for an ideal ML detector is prohibitive for large spreading matrices. We therefore postulate that the best compromise between capacity and performance is to use high-order alphabets such as 16QAM in preference to high-order block spreading matrices such as \mathbf{R}_4 .

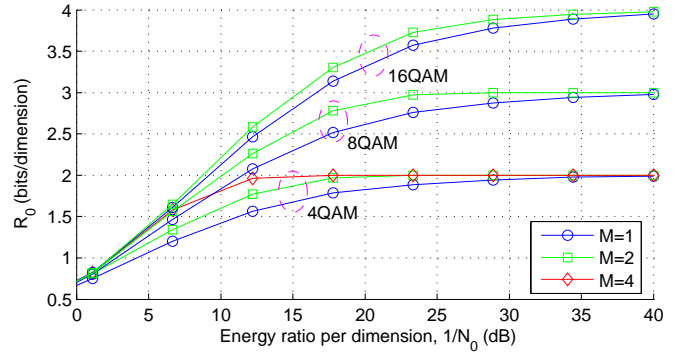


Fig. 5. Cutoff rate R_0 in CM2.

Order	Bits per Symbol	States	
$M = 1$	2	4QAM	4
$M = 2$	2	4QAM	16
$M = 4$	2	4QAM	256
$M = 1$	3	8QAM	8
$M = 2$	3	8QAM	64
$M = 1$	4	16QAM	16
$M = 2$	4	16QAM	154

TABLE I

COMPLEXITY WITH REGARD TO SPREADING MATRIX AND SYMBOL ALPHABET.

To validate this theory, Fig. 6 uses a Monte-Carlo simulation to investigate the benefits of applying DCM to several symbol alphabets. The channel model are packet length remain as CM2 and 1500 octets respectively. To maintain the 480Mbps data rate used in our previous simulation, more coded bits are needed for the 8QAM and 16QAM symbol alphabets. This is easily achieved by modifying the puncturing pattern as per Table II. Similar to the MB-OFDM standard [10], these puncturing patterns are expressed in terms of blocks of 9 coded bits. In other words, each group of 3 information bits, $\{A, B, C\}$, are applied to a $R = \frac{1}{3}$ convolutional coder to produce 9 coded bits $\{A_0, A_1, A_2, B_0, B_1, B_2, C_0, C_1, C_2\}$. The puncturing pattern the determines which of these coded bits are discarded. At the receiver, any discarded bits are reinstated as soft-decision-neutral dummy-data before Viterbi decoding. In other words, with 4QAM, 8QAM and 16QAM utilizing 2, 3 and 4 bits-per-symbol at coding gains of $\frac{3}{4}$, $\frac{1}{2}$ and $\frac{3}{8}$ respectively, we maintain a constant allocation of 1.5 information bits-per-symbol.

The results of Fig. 6 suggest that the coding gain for a punctured $R = \frac{3}{4}$ convolutional code is insufficient to reliably recover from the severe frequency-selective fading in the CM2 channel. Although DCM improves performance by mitigating the worst of these fades, the 2-point frequency-diversity does not fully compensate for the insufficient coding gain.

To more accurately estimate real-world performance, Fig. 7 shows the impact of using the simplified ML detector of (4) for both unspread 16QAM and DCM 4QAM. We note that the simplified ML detector has no impact on 4QAM DCM. This is to be expected given that the simplicity of the

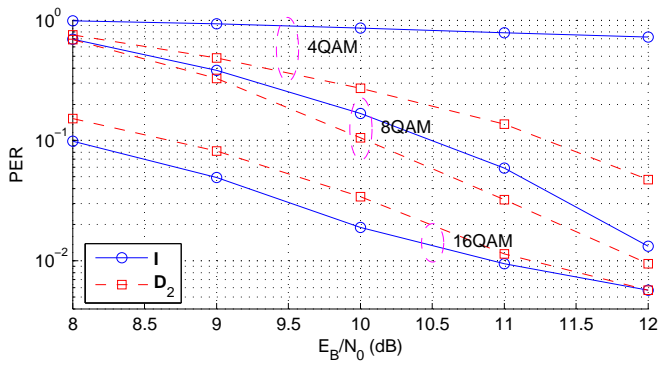


Fig. 6. PER at 480Mbps in CM2 for several symbol alphabets.

Order	Coding Rate	Transmitted Bits
4QAM	$R = \frac{3}{4}$	$\{A_0, B_0, C_1, C_2\}$
8QAM	$R = \frac{3}{4}$	$\{A_0, A_1, B_0, B_1, C_1, C_2\}$
16QAM	$R = \frac{3}{8}$	$\{A_0, A_1, A_2, B_0, B_1, C_0, C_1, C_2\}$

TABLE II

PUNCTURING PATTERNS FOR 480Mbps WITH REGARD TO CONSTITUTION ORDER.

underlying 4QAM symbol alphabet. Conversely, the simplified ML detector reduces the performance of unspread 16QAM at higher SNR. However, since the MB-OFDM standard targets a PER of 8%, practical SNRs will be so small that these losses are trivial.

V. CONCLUSIONS

By considering the complexity estimates of Table I in conjunction with the PER of Figs. 6 and 7, we conclude that a 16QAM symbol alphabet with an $R = \frac{3}{8}$ punctured convolutional code is the most effective way for MB-OFDM to obtain a 480Mbps data rate. We also conclude that simplified ML LLR soft-decision outputs are a computationally feasible means of receiving high data rate transmissions in frequency-selective channels. We found that up to a 2 dB advantage over the MB-OFDM standard's current approach of DCM-spread 4QAM can be achieved at no increase to complexity. In addition, we found that an 8QAM or 16QAM constellation can be supported using existing convolutional coders and Viterbi decoders as the necessary adjustments to the coding rate can be accommodated by modifying the puncturing pattern.

REFERENCES

- [1] K. Siwiak and D. McKeown, *Ultra-wideband Radio Technology*. Chichester, England: Wiley and Sons, 2004.
- [2] *First Report and Order, Revision of Part 15 of the Commission's Rules Regarding Ultra-Wideband Transmission Systems*, Federal Communications Commission ET Docket 98-153, Feb. 2002.
- [3] A. Batra, J. Balakrishnan, G. R. Aiello, J. R. Foerster, and A. Dabak, "Design of a multiband OFDM system for realistic UWB channel environments," in *IEEE Transactions on Microwave Theory and Techniques*, vol. 52, no. 9, Sept. 2004, pp. 2123–2138.
- [4] A. Batra and J. Balakrishnan, "Improvements to the multi-band OFDM physical layer," in *Proceedings of the 3rd IEEE Consumer Communications and Networking Conference*, vol. 2, Jan. 2006, pp. 701–705.

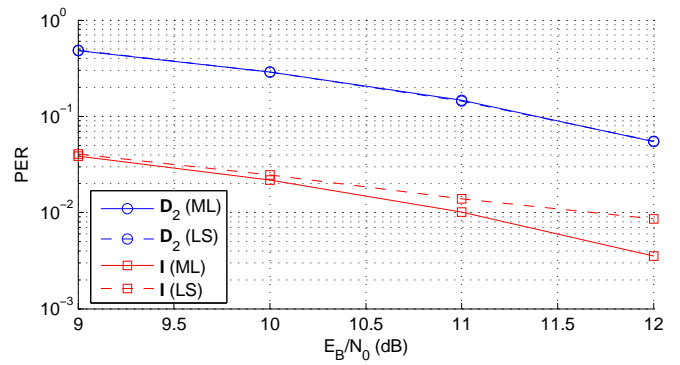


Fig. 7. PER at 480Mbps in CM2 for ML vs LS estimation.

- [5] E. Viterbo and J. Boutros, "A universal lattice code decoder for fading channels," *IEEE Trans. Inform. Theory*, vol. 45, no. 7, pp. 1639–1642, July 1999.
- [6] A. Bury, J. Engle, and J. Linder, "Diversity comparison of spreading transforms for multicarrier spread spectrum transmission," *IEEE Trans. Commun.*, vol. 51, no. 5, pp. 774–781, May 2003.
- [7] J. G. Proakis, *Digital Communications*, 3rd ed. New York: McGraw-Hill Book Company, 1995.
- [8] M. McCloud, "Analysis and design of short block OFDM spreading matrices for use on multipath fading channels," *IEEE Trans. Commun.*, vol. 53, no. 4, pp. 656–665, Apr. 2005.
- [9] A. F. Molisch, J. R. Foerster, and M. Pendergrass, "Channel models for ultrawideband personal area networks," *IEEE Wireless Commun. Mag.*, pp. 14–21, Dec. 2003.
- [10] *High Rate Ultra Wideband PHY and MAC Standard*, ECMA International ECMA-368, Dec. 2005.